Cholesteric textures observed by transmission electron microscopy in diffraction contrast

J. Pierron, A. Boudet, P. Sopena, Michel Mitov, P. Sixou

Accepted version published in: *Liquid Crystals*, **19**, 257-267 (1995)

Cholesteric textures observed by transmission electron microscopy in diffraction contrast

J. PIERRON, A. BOUDET, P. SOPENA

CEMES-LOE (CNRS UPR 8011), BP 4347, F-31055 Toulouse Cedex, France

M. MITOV* and P. SIXOU

Laboratoire de Physique de la Matière Condensée (CNRS UA 190),

Université de Nice-Sophia Antipolis, Parc Valrose, F-06108 Nice Cedex 2, France

Article history: Received 26 July 1994. In final form 7 December 1994. Accepted 7 February 1995

https://www.tandfonline.com/doi/abs/10.1080/02678299508031977

We have studied the structure of a side chain cholesteric macromolecule by transmission electron microscopy. Up to now, the structure of cholesteric polymers has usually been studied by optical microscopy, and sometimes by scanning electron microscopy, but rarely by transmission electron microscopy, because of the difficulty of obtaining an image of the texture without radiation damage.

In this paper we compare the morphologies obtained in specimens prepared from solution and in ultramicrotomed specimens. The small thickness of the sample prepared from solution and the influence of the carbon film oblige the cholesteric axis to lie in the substrate plane. The dark and bright lines therefore form various patterns, such as fingerprints and spirals, with edge dislocations and different types of π disclinations.

The existence of a contrast of dark and bright lines related to the cholesteric periodicity in sections obtained by ultramicrotomy is not well understood. In this paper, we also investigate the contribution of three types of contrast (orientation of a single molecule, thickness modification under radiation and diffraction contrast). From the evidence of electron diffraction patterns, dark field and bright field images in transmission electron microscopy, we demonstrate that diffraction contrast is a contributing mechanism in undamaged samples prepared from solution or by ultramicrotomy. In ultramicrotomed samples, this contrast quickly fades away during the observation, while another contrast due to the electron radiation appears. The orientation of the molecule is not relevant.

We also demonstrate that the diffraction contrast of the dark lines in bright field is due to an intermolecular distance of 4·7 Å oriented along the cholesteric axis. This is in agreement with the traditional image of a cholesteric, in which the mesogenic molecules lie perpendicular to the cholesteric axis.

1. Introduction

The rapid expansion of research on side chain liquid crystals polymers (SCLCPs) and of their applications requires an understanding of the relation between their structures and their properties. These polymers consist of a backbone chain to which mesogenic side groups are attached. These mesomorphic phases result from the compromise between the tendency to mesomorphic organization of the side groups and the flexibility of the backbone chain and of the spacers [1]. This mesomorphic structure is responsible for the dielectric and optical properties of the polymers.

In this paper, we study the cholesteric structure of a side chain macromolecule by transmission electron microscopy. This molecule is a cyclic copolysiloxane with two side groups, a biphenyl-4-yl 4-allyloxybenzoate and a cholesteryl 4-allyloxybenzoate (see figure 1), as described in § 2. The phase diagram of the blend of this compound with a low molar mass nematic material has already been studied in a previous paper [2].

Cholesteric molecules have been widely studied by optical microscopy [3], and characterized by their specific textures, such as focal-conics. When the cholesteric axis is in the substrate plane, fingerprint-like texture and spirals can also be seen [4, 5]. They are made of curved parallel lines, a half pitch apart and exhibit characteristic defects such as disclinations. However, these periodic lines are seen only if the pitch is higher than about 1 μm. If not, the use of electron microscopy is compulsory.

By means of scanning electron microscopy (SEM) [6, 7], well-oriented lines due to a periodic relief have been seen on freeze fractured specimens of cholesteric

*Email address : mitov@cemes.fr

Accepted version published in: *Liquid Crystals*, **19**, 257-267 (1995)

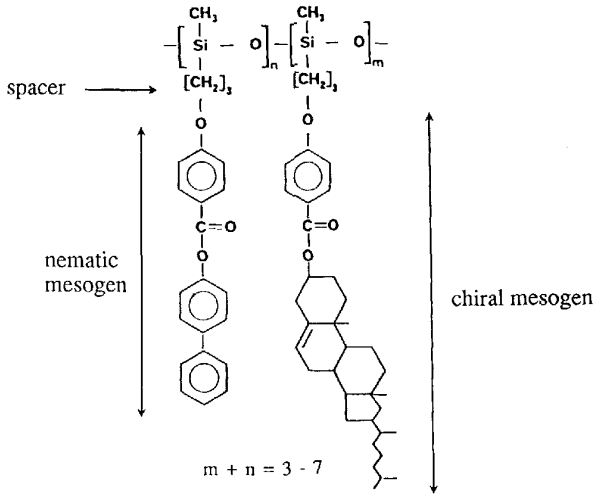

Figure 1. Formula for the cholesteric cyclic copolysiloxanes.

polymers. The periodicity was identified with the cholesteric pitch. The same periodic relief of parallel lines has also been observed by atomic force microscopy [8].

To observe cholesteric mesophases in transmission electron microscopy (TEM), the freeze fracture technique has rarely been used [9, 10], though successful for lyotropic phases [11]. Such pictures show a periodic contrast directly related to the cholesteric periodicity, displaying some disclinations.

Specimens obtained by ultramicrotomy also show dark and bright lines [6–8, 12–14] related to the periodicity with characteristic patterns, edge dislocations and π disclinations [6–8, 13]. One part of this paper is devoted to the investigation of textures such as fingerprints and disclinations. These could be observed in ultramicrotomed specimens, but we obtained a larger variety of figures with specimens prepared from solution, including fingerprints, spirals, disclinations and edge dislocations.

The existence of such a contrast in microtomed sections is rather surprising and not well understood. For freeze fractured specimens, it is reasonable to think that this contrast is due to differences in thickness, or the shadowing by evaporation of heavy metals at low angles, whereas the contrast in TEM could be explained either by a difference in orientation of the molecules [6, 13], a difference in thickness in the section, or by diffraction contrast. The difference in thickness could be due to sectioning artefacts [12], or to electron radiation [8].

In this paper, we have two objectives. First, we compare the morphologies obtained in solution-prepared specimens and in ultramicrotomed specimens, and we study the shapes and the frequencies of disclinations and dislocations. Second, we demonstrate the role of diffraction contrast in undamaged specimens in transmission electron microscopy. We show how it is taken over during our observation by the radiation contrast, associated with modification of the thickness. Our calculations indicate that the orientation of individual molecules has no perceptible influence. By means of bright-field images, dark-field images and electron diffraction patterns in solution-prepared specimens, we investigate how the mesogenic molecules are arranged with respect to the cholesteric axis and the periodic lines and show that this disposition is in accordance with the usually accepted model.

2. Experimental

2.1. *Materials*

The macromolecules studied are side chain cyclic copolysiloxanes synthesized by Dr F. H. Kreuzer [15–17]. Two types of mesogenic side groups are attached to the cyclic backbone via alkyl flexible spacers: the *n* biphenylyl groups confer a nematic tendency and the *m* cholesteryl groups a cholesteric character (see figure 1). The number of siloxane units varies between 3 and 7 with 5 being the most common value, so that the term 'macromolecule' is more appropriate than 'polymer'. The selective reflection wavelength (of Bragg type), and therefore the helical pitch, depend on the mole fraction of the chiral component. When the *m*/*n* ratio increases, the pitch decreases and the selective reflection goes from red to blue. Four macromolecules have been studied (see table 1), the reflection wavelength is adjustable by mixing these four basic materials. As polymeric materials, cyclic siloxanes offer an advantage over low molar mass compounds in that the required cholesteric mesophase may be attained by annealing at high temperature and locking the phase into a glassy matrix by athermal quenching. The glass transition takes place between 40°C and 55°C and the cholesteric–isotropic transition at 180–200°C. Possible applications of these orientable liquid crystal copolysiloxanes are optical data storage [18], optical notch filters (capable of rejecting incident optical radiation in a selected wavelength range, while transmitting it out of this region) [19], or the decorative sector [20]. When they are put in solution in a low molar mass nematic liquid crystal, the

Table 1. Some physical properties of the cyclic copolysiloxanes (from [2]).

Cholesteric copolysiloxanes	red	gold	green	blue
Cholesteric pitch/nm	370	345	315	290
Reflection wavelength/nm	675	595	540	450
Glass transition temperature/°C	40/50	43/53	45/55	40/50
Clearing temperature/°C	180/210	id.	id.	id
Processing temperature/°C	140/170	id.	id.	id.

resulting material can present, by varying the temperature and concentration parameters, a selective reflection covering the visible spectrum [2]. When a large pitch cholesteric resulting from these mixtures is subjected to an electric field, it can exhibit a nucleation and the growth of spiral patterns [2, 21].

2.2. *Sample preparation for transmission electron microscopy*

We have used two techniques to prepare the specimens for TEM—ultramicrotomy and dissolution.

In the first technique, the sample was melted between two glass slides for 12 h at 160°C below the cholesteric–isotropic transition, and then slowly cooled (1°C min^{-1}). The thickness of the sample was determined by additional glass slides placed between the lower and upper glass slides. Ultrathin sections were then prepared from the bulk material with an ultramicrotome (Reichert Om U3 and Ultracut S) using a diamond knife. However, ultramicrotomy can cause mechanical deformations as has been demonstrated for smectic polymers [22].

The other technique consists in dissolving the macromolecule in dichloromethane at 10 wt % concentration. A drop of this solution was put on a carbon coated grid and allowed to dry. These specimens did not exhibit typical cholesteric dark and bright lines. In order to favour the cholesteric structure, the specimens were therefore subjected to the same thermal process as in the previous preparation. The thickness of the sample can be varied by altering the concentration of the solution.

2.3. *Transmission electron microscope observations*

Transmission electron microscope observations were carried out with Philips CM20 and Jeol 200 CX microscopes operating at 200 kV. As for all crystalline polymers, the resolution is limited by radiation damage [23, 24]. In our conditions of very low incident beam intensity, the ordered diffraction patterns disappear within about 1 mn (no measure of the incident intensity could be made). To study the diffraction contrast, micrographs were taken on areas not previously exposed to the electron beam and we ensured that the diffraction pattern was not altered after the exposure. Dark field images could also be obtained with the CEMES high voltage electron microscope operated at 2 MV. The use of high voltage decreases the radiation damage and permits longer observation times in diffraction contrast [25].

3. Morphology and defects

3.1. *Samples obtained from ultramicrotomy*

We observed alternate dark and bright lines, as in studies by other authors [6–8, 12–14]. Straight lines define large domains with few dislocations (see figure 2).

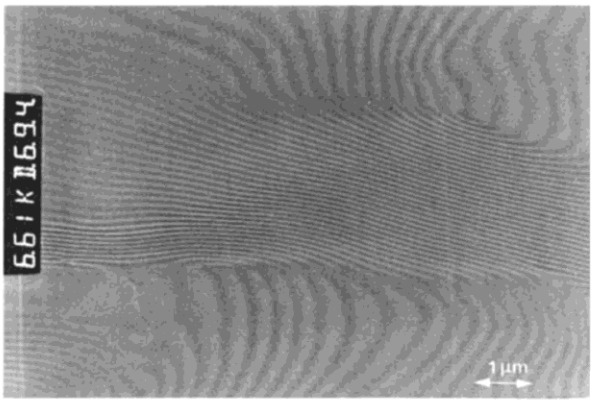

Figure 2. Sample prepared by ultramicrotomy. Silicone blue. Bright-field image in TEM.

Domains with different orientations are contiguous. At the boundary between two domains, the lines abruptly change their orientation but remain continuous.

The periodicity of the lines varies from one domain to another. This is an indication of a variation in the orientation of the cholesteric axis. In the bulk, not too close to the glass slide surfaces, the axis is free to develop in any orientation, and may therefore lie out of the plane of the section. As the thickness of our sample may reach 1mm, the influence of the surface is negligible and domains can develop freely. It is possible that during annealing between the glass slides, a slight flow of the material also occurs, which could induce a local orientation in different parts of the specimen.

Some authors have also seen regions departing from a uniform orientation [8]. Typical fingerprint textures, which have been observed by some other authors [4–6], are absent in our ultramicrotomed specimens. They are however frequent in solvent prepared specimens, as reported in the next section.

3.2. *Specimens obtained from solution*

The four macromolecular specimens show the typical contrast of dark and bright lines shown in figures 3 and 4. Owing to radiation damage, the contrast decreases after a short time. This loss of contrast will be investigated in part 4. The micrographs shown in figures 3 and 4 were taken before any decrease of contrast, like all the other pictures in this section (see figures 3 to 10).

The distances between the lines are nearly constant and correspond to half of the values of the pitch already known from [2] (see table 2). This indicates that the cholesteric axis lies roughly in the substrate plane.

The textures are well defined and striking. The cause may be the small thickness of the specimen, thinner than the usual slices obtained by ultramicrotomy ($< 0{\cdot}1$ µm), but it has not yet been possible to measure this thickness.

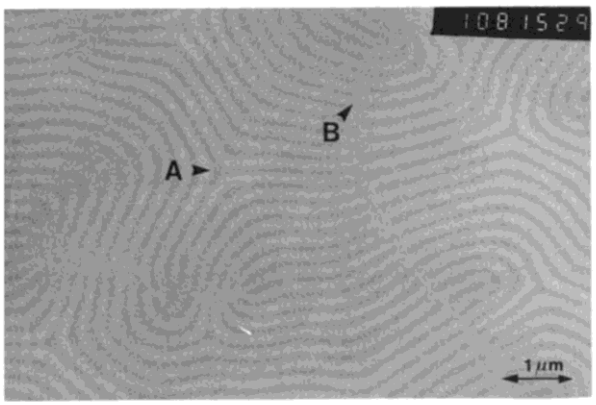

Figure 3. Fingerprint texture. Silicone red. (A) $-\pi$ disclination; (B) edge dislocation with interruption of the lines. Sample prepared from solution. Bright-field image in TEM.

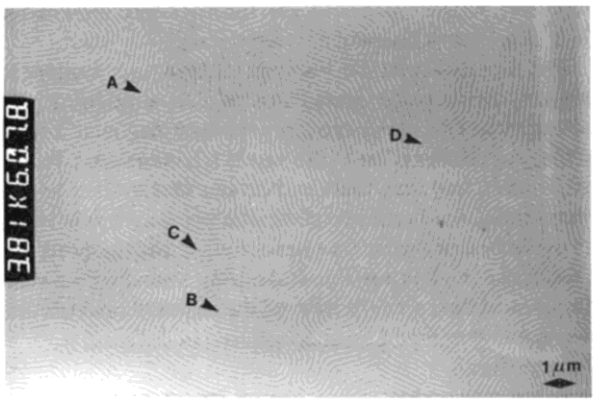

Figure 4. Fingerprint texture. Silicone red. (A) $-\pi$ disclination; (B) $+\pi$ disclination; (C) edge dislocation; (D) disclination with interruption of the lines. Sample prepared from solution. Bright-field image in TEM.

Another possible cause is the influence of the carbon and the air surface. In the solution, the molecules are confined in a limited thickness, which is close to the value of the pitch (0·3 μm). We have no indication of the type of surface constraint on the molecules for such a geometry, but it could be the reason why the cholesteric axis lies parallel to the substrate.

The lines are almost everywhere parallel, and several textures are observable. In small areas, these lines are perfectly straight and no defect can be seen. These areas are located beside the edge of the copper grid bar.

The most frequent texture is the fingerprint. It is characterized by numerous sinuous lines which can have any orientation in the sample plane (see figures 3 and 4). Numerous disclinations and edge dislocations can be identified (see figures 3 and 4). The sketch in figure 5 shows the four disclination types that have been observed.

Table 2. Values of the distances measured between the lines compared to the cholesteric pitch (from [2]). $\bar{d}$ are the average distances between the lines.

Substances	Distance between lines d/nm	Cholesteric pitch/nm
Silicone blue	$140 < d < 180$ $\bar{d} = 160$	290
Silicone green	$150 < d < 200$ $\bar{d} = 165$	315
Silicone gold	$150 < d < 190$ $\bar{d} = 175$	345
Silicone red	$150 < d < 250$ $\bar{d} = 200$	370

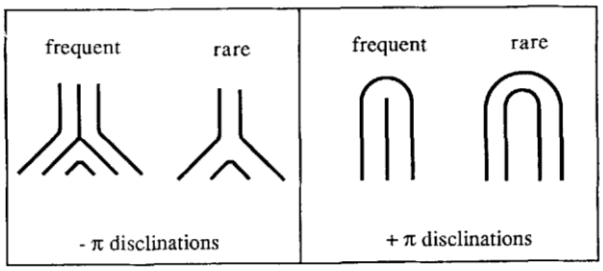

Figure 5. Sketch of the types of disclination observed and their relative frequencies.

Two are of positive sign and two of negative sign [26]. The disclinations of positive sign appear more frequently, as already observed by Davé in ultramicrotomed specimens [7]. Some authors [6, 7] have identified disclinations with a dark line core as τ-type disclinations, and disclinations with a bright line core as a λ-types. These authors observe that the frequency of occurrence of the λ disclination cores (white line) is greater than the frequency of the τ disclination cores (dark line), and they calculate that the λ disclinations need less energy [26]. We have found the contrary: the disclinations with a dark line core are more frequent. This could be due to the influence of the forces of the free surface and of the carbon substrate surface which has to be taken into account in the calculation of the energy.

Some edge dislocations are observed (see figures 3 and 4). They consist of two associated disclinations of opposite sign. The different associations between $+\pi$ and $-\pi$ disclinations and their frequencies are shown in figure 6. The distance d between the cores of two paired disclinations falls between a half pitch and three times the pitch, giving rise to twice as many supplementary lines.

We have also observed areas in which the lines are interrupted and form a disclination (see figure 4). In one case, the disclination extended along a curve (see figure 3), the alternate dark and bright lines lying perpendicular to it. The number on either side is not the same, as it is for

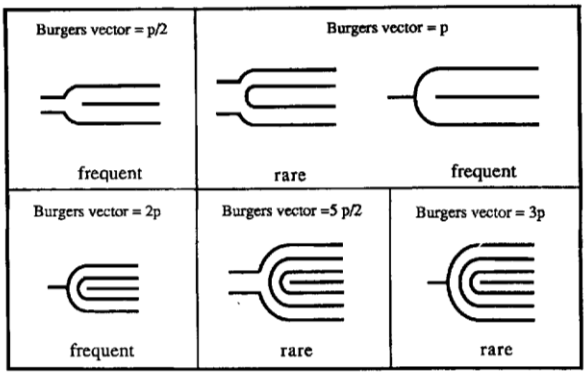

Figure 6. Sketch of the types of edge dislocations observed and their relative frequencies. p = cholesteric pitch.

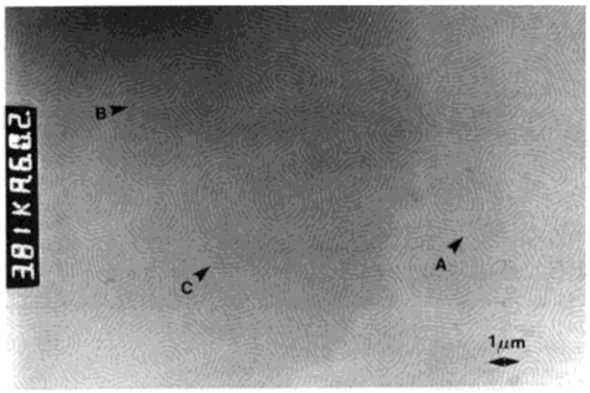

Figure 7. Spiral texture and disclinations. Silicone blue. (A) $-\pi$ disclination; (B) $+\pi$ disclination; (C) edge dislocation. Sample prepared from solution. Bright-field image in TEM.

an edge dislocation, but here it is not due to the association of two disclinations of opposite sign.

Another texture consists of numerous double spirals (see figure 7), elongated in any direction in the sample plane. The contrast variations of the background are due to thickness variations in the sample. The spirals are very often left-handed. They are bounded by their contacts with their neighbours. These boundaries give rise to numerous disclinations, which permit the spirals to be matched (see figure 7). Their size depends on the distance between their cores. The length of the long axis is about 1 to 5 μm. The different arrangements of the lines at the centre of the spirals are depicted in figure 8. Type A is common, the others are more rare.

A last texture was exceptionally observed in areas of no specific location. It is characterized by short and very wavy bright and dark lines (see figure 9). The number of disclinations in this texture is greater than in the other textures. The number of lines that are parallel is never greater than ten, and they stay parallel only over short distances.

Finally, some rare areas of no specific location show two families of superimposed dark and bright lines (see figure 10). There is no relation of orientation between the two families and it seems that two decorrelated layers are superimposed without disturbing each other. We do not know how this is possible. Two films could be formed successively during the evaporation process.

3.3. *Comparison of the two types of specimens*

With respect to the morphology in bulk specimens, the textures of solvent-prepared specimens display a wider variety of figures such as fingerprints. The occurrence of spirals had not been observed previously in such material, though it had been seen in thick specimens of small molecule liquid crystal materials by light microscopy [5]. The explanation depends on an understanding of the origin of contrast in electron microscopy, and we consider this in the next section.

Solution of the sample is a very simple way of preparing specimens for transmission electron microscopy. It gives regular and reproducible results.

The preparation method does of course influence the structure. The role of the surfaces is complex but it is clear that it must be taken into account to explain the following features of the morphology: the cholesteric axis lies in the substrate plane; there are many spirals; the frequencies of λ- and τ-type disclinations are the reverse of what is observed by other authors in bulk specimens.

4. Factors influencing the contrast

Three factors have already been suggested to explain the contrast of bright and dark lines of cholesteric substances in transmission electron microscopy. One is diffraction contrast and we demonstrate below that this occurs in undamaged solution-prepared samples. Bright spots of the diffraction pattern are selected or excluded by the aperture to form the image, so that this contrast is mainly related to the lattice of centres of gravity of the molecules. The diffracted intensity is also modulated by the molecular factor that depends on the nature, form and orientation of the single molecules positioned on these centres of gravity, and could be a second cause of contrast. The influence of the orientation of the mesomorphic side groups with respect to the incident electrons has already been suggested [6, 8, 13] as a contributing factor. We calculate here than the influence of the orientation of an individual molecule is negligible.

A third factor is a variation in thickness of the sample, which decreases with the electron irradiation [8]. We report below that this has an effect in microtomed specimens, but not in solution-prepared samples. This

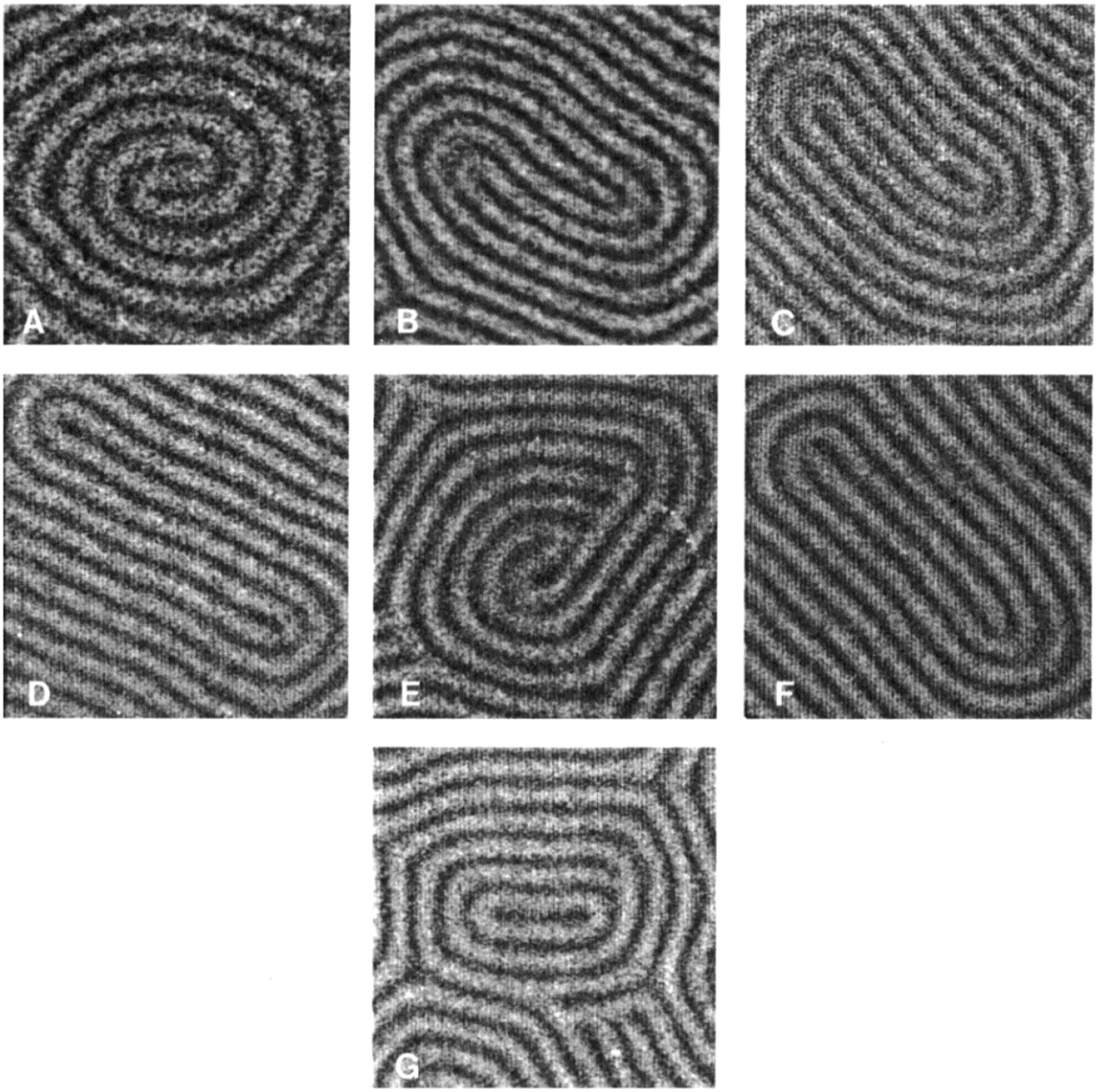

Figure 8. Different types of spirals. Bright-field images in TEM, processed in order to increase the contrast.

could be due to a difference in thickness between the two types of preparations.

4.1. *Electron diffraction contrast*

The electron diffraction patterns of the four macromolecules prepared in solution (see figure 11 (*b*)) consist of two fairly broad rings. In nematic and smectic substances, they are interpreted as the distribution of lengths and orientations of the distances between the molecules. It is likely that the scattering units in this cholesteric macromolecule are the mesogenic side chains. The distribution of their centres of gravity is intermediate between a crystalline distribution and a completely amorphous one. These rings quickly fade away and change into broad amorphous rings as radiation damage proceeds. The corresponding distances in direct space were evaluated as $4{\cdot}7 \pm 0{\cdot}4$ Å for the first ring, by scanning the diffraction patterns in a microdensitometer. The second

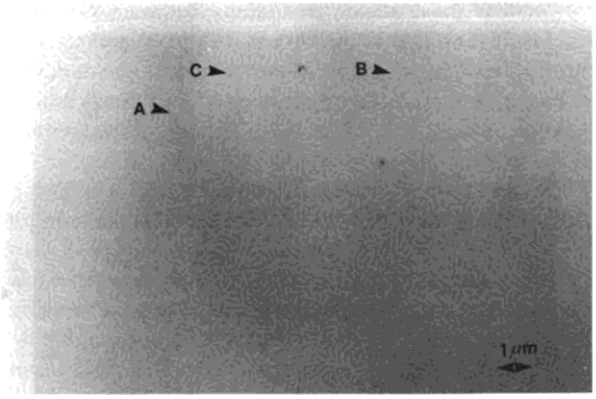

Figure 9. Flake texture. Silicone blue. (A) $-\pi$ disclination; (B) $+\pi$ disclination; (C) edge dislocation. Sample prepared from solution. Bright-field image in TEM.

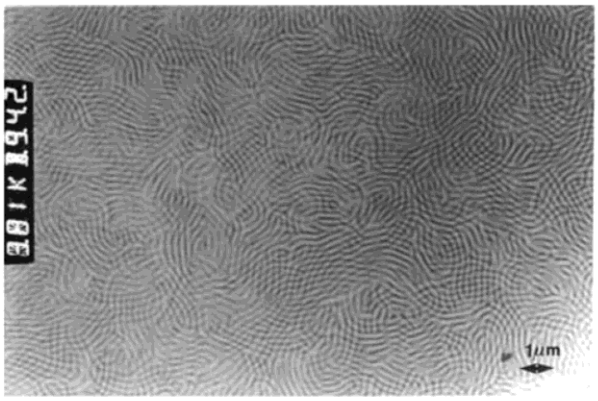

Figure 10. Superimposed line networks. Silicone gold. Sample prepared from solution. Bright-field image in TEM.

ring is a second peak in the transform of the distribution, but not a second order ring in the sense of crystalline order. To understand the implication of the diffraction contrast on the dark and bright lines, we tested the influence of the size of the contrast aperture, including or excluding the first diffraction ring, in several bright field images of the same area of a sample prepared from solution. The dark lines are well contrasted when the size of the contrast aperture is smaller than the first diffraction ring, and fade away, but do not disappear, when a larger contrast aperture is used, including or excluding the second diffraction ring. It is then obvious that the dark line contrast, observed on undamaged samples, is directly related to the diffraction ring in the 4·7 Å range.

The fact that a diffraction mechanism is operating is confirmed by dark-field images and their evolution with radiation damage. Dark-field images have been performed with the CEMES high voltage electron microscope operated at 2 MV. The use of such a high voltage increases the lifetime of the diffraction contrast, so that it was easier to obtain micrographs than at 200 kV. The selected beam was a portion of the first diffraction ring, defined by a scattering vector **S**, so that the areas which appear bright on the image are those diffracting with the periodicity and the orientation defined by **S** (see figure 11). As expected, the lines which appeared bright in dark field are among those which were dark in bright field. The contrast in bright

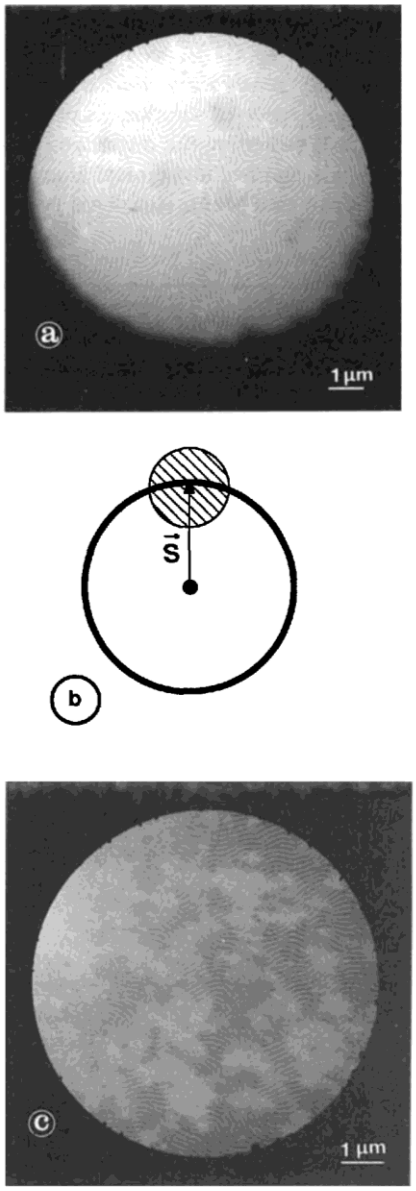

Figure 11. Bright-field (*a*), diffraction pattern (*b*) and dark-field (*c*) from the same area in a sample prepared from solution. The circle indicates the **S** scattering vector used to form the dark-field. Silicone blue. TEM at 2 MV.

field and in dark field rapidly disappears during radiation damage, as reported in § 4.2.

With the aid of electron diffraction patterns and dark-field and bright-field images in transmission electron microscopy of solution-prepared specimens, we have thus demonstrated that the 4·7 Å ring was responsible for appearance of the dark lines in undamaged samples (in bright field) and did not intervene in the bright lines. In § 5, we discuss how the mesogenic units are capable of accounting for this mean distance.

4.2. *Irradiation contrast*

During the observation of solution-prepared specimens under the electron radiation, the diffraction rings widen, lose their intensity and become typical amorphous rings, as is usual for diffracted beams in ordered polymers. This means that the distance periodicity between two units (molecules) related to the ring is destroyed and replaced by an amorphous disorder. At the same time, the dark lines in bright field (and the bright lines in dark field) quickly become faint and disappear. No thickness contrast remains in the lines.

On the contrary, in the case of samples prepared by ultramicrotomy, an increase in the contrast is seen, despite the widening and the decrease in intensity of the electron diffraction rings. The diffraction contrast disappears, and a different type of contrast appears, as already observed by Bunning *et al.* [8]. They have shown that this is due to a variation of thickness of the section which occurs during the specimen irradiation.

We assume that irradiation acts as a differential etching to produce thickness variation of the sample during

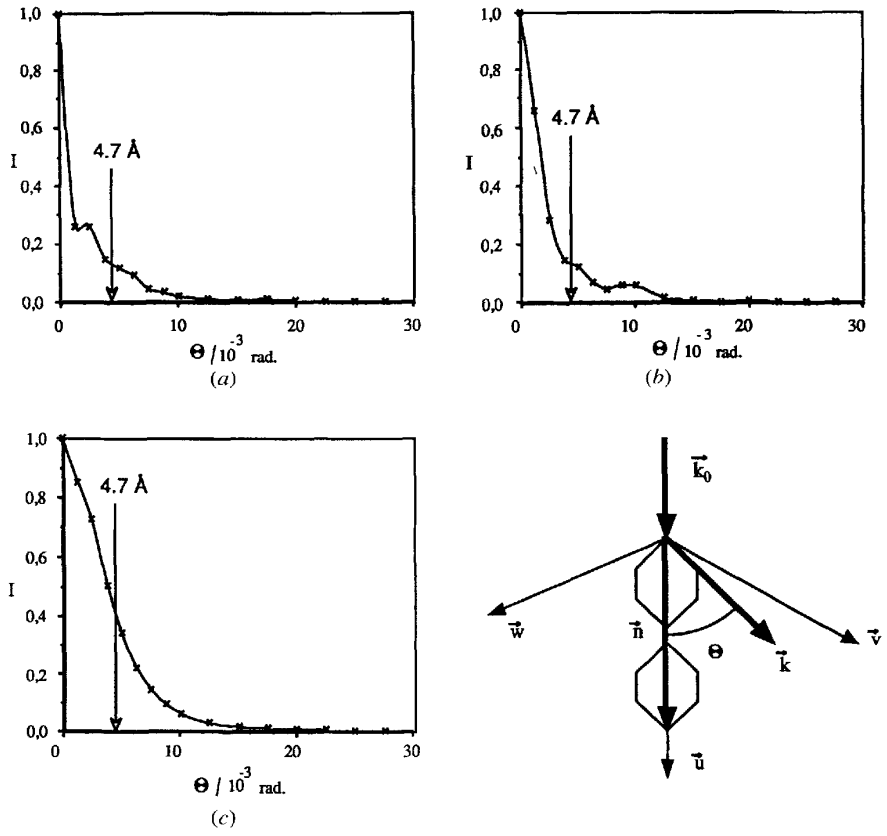

Figure 12. Scattered intensity, I, as a function of the scattering angle, θ, calculated in the kinematical approximation. $\mathbf{k}_0$: incident beam. $\mathbf{k}$: scattered beam. $\mathbf{n}$ is parallel to the long axis of the biphenylyl group. I is calculated for three orientations of the incident beam $\mathbf{k}_0$ with respect to the biphenylyl group: (*a*) $\mathbf{k}_0 /\!/ \mathbf{u}$, the long axis of the group is parallel to the incident beam. The results are identical for $\mathbf{k}$ in the plane $(\mathbf{u}, \mathbf{v})$ or $(\mathbf{u}, \mathbf{w})$. (*b*) $\mathbf{k}_0 /\!/ \mathbf{v}$. The long axis of the group is perpendicular to the incident beam. The results are identical for $\mathbf{k}$ is in the plane $(\mathbf{u}, \mathbf{v})$ or $(\mathbf{v}, \mathbf{w})$. (*c*) $\mathbf{k}_0 /\!/ \mathbf{w}$. The long axis of the group is perpendicular to the incident beam. The results are identical for $\mathbf{k}$ is in the plane $(\mathbf{u}, \mathbf{w})$ or $(\mathbf{v}, \mathbf{w})$.

observation. It is known from studies involving polyethylene crystals that the effect of the electrons usually increases when they go deeper into the specimen, with a maximum at a small distance from the surface, in the 20–100 nm range [25]. It is likely that the channelling of the electrons along columns of aligned molecules likewise increases with the depth, but we do not know how it increases with the thickness. In our samples obtained by ultramicrotomy, the thickness is about 50 nm. The fact that the thickness variation is not observable on solution-prepared samples may indicate that they are thinner, as already mentioned above.

4.3. *Influence of the molecular orientation on the contrast*

We now consider why the dark lines contribute more to the diffraction ring than the bright lines, as demonstrated in § 4.1. This may be due to a different distance distribution or to a different molecular scattering factor. We now examine the influence of this second factor. It is known that the diffraction pattern intensity in reciprocal space is, in a first approximation, the product of the distance distribution factor and the molecular factor. The distance distribution factor is due to the positions of the centres of gravity of the repeating unit (a molecule or a unit cell). It reflects the mean distance and the alignment directions of these centres and gives rise to the diffracted rings with their specific distances. If the mean distance has an effect on the difference between dark and bright lines, we need to examine why there is a 4·7 Å distribution in dark and not in bright lines. If the molecular factor is indeed relevant, it should be different when the molecule is tilted with respect to the electron beam.

To check this hypothesis, we have calculated the intensity of the scattered electron beam for three orientations of a biphenylyl group (see figure 12). The scattered intensity of a set of a limited number of atoms in the kinematical approximation is

$$I = \sum_j |F_j|^2 + \sum \sum_{j \neq k} F_j F_k \exp i2\pi \mathbf{S} \mathbf{r}_{jk}$$

where the F_i are the scattering coefficients for electrons [27], and **S** is the scattering diffraction vector, defined by $\mathbf{S} = \mathbf{k} - \mathbf{k}_0$ where $\mathbf{k}_0$ and **k** are, respectively, the incident and the scattered beams.

The long axis of the biphenyl molecule is parallel to the unit vector **u** with the flat phenyl rings in the (**u**, **v**) plane. The incident beam $\mathbf{k}_0$ was chosen in each of the three directions of the vectors **u**, **v** or **w**. The intensity was then calculated as a function of the angle θ for two directions of **k** situated in two perpendicular planes containing the unit vector $\mathbf{k}_0$. The two curves obtained are similar for each of the three orientations of the incident beam $\mathbf{k}_0$. There is no peak in the range corresponding to the 4·7 Å distance in direct space. Nevertheless, in the same range, when the group is perpendicular to the incident beam, the scattered intensity is four times greater when the incident beam is parallel to the vector **w** than to **v**. When the group is parallel to the incident beam ($\mathbf{k}_0$ parallel to **u**), the scattered intensity is of the same order of magnitude as when the incident beam is parallel to **v**.

From this we concluded that there is no effect of the orientation of the group on the molecular factor. The difference between dark and bright lines must come from the distance distribution factor. A question therefore remains to be answered: why is this distance distribution different in dark and bright lines?

5. Intermolecular distance

We now investigate the origin of the 4·7 Å distance between the scattering units and its orientation in the dark lines.

We could obtain diffraction patterns from areas as small as 80 μm^2, including only four dark, and four bright lines. They consist of two symmetrical crescents placed on the same diameter. This means that the scattering units are locally preferentially oriented. When the direction of the crescent radius is plotted on the corresponding bright field image, it is found to be perpendicular to the line, so that the 4·7 Å distance between two units is perpendicular to the direction of these lines (see figure 13). The same electron diffraction patterns were found in samples prepared by ultramicrotomy.

On the dark-field images, the lines that appear bright in dark field are among those which were dark in bright field. But only those that are perpendicular to **S** (see figure 13) are bright, while the lines that are not perpendicular to the selected direction **S** appear dark and are located in an area where the contrast is lost. These observations demonstrate first that the inter-unit distances are located only in the bright lines in dark field (which are the dark lines in bright field) and give rise to the crescents, and second, that **S** (the periodicity) is perpendicular to these lines, that is to say, along the cholesteric axis.

This suggests that this periodicity is the distance between the side chains of the macromolecules, because this is in agreement with the traditional image of a cholesteric, in which the molecules lie perpendicular to the cholesteric axis [1]. Furthermore, the 4·7 Å distance is in the range of the real distance between the side chains in the macromolecules. As in nematics, the crescents in the dark lines indicate that the chains are on average perpendicular to the beam and lie in the substrate plane.

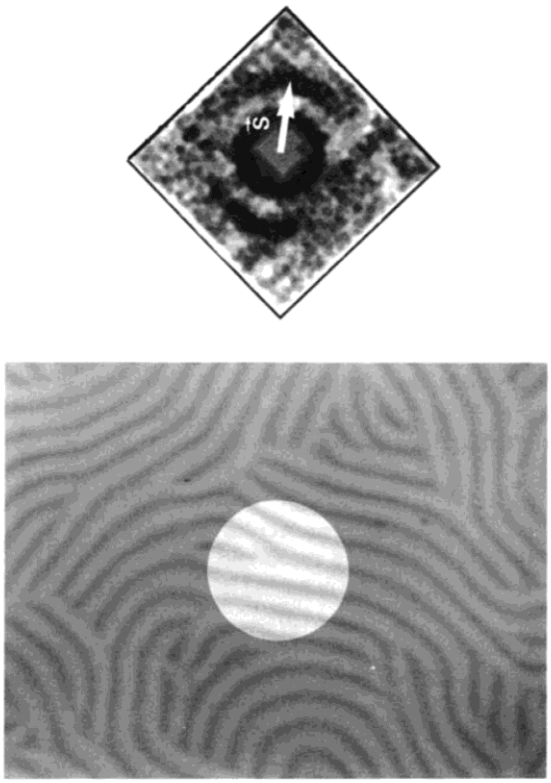

Figure 13. Oriented local electron diffraction of the silicone blue and the bright-field image of the corresponding area. The electron diffraction pattern has been processed to increase the contrast.

This could be verified by tilting the specimen around an axis parallel to the lines. Chains not in the plane could then be brought into it, so that the dark lines would move with respect to the specimen. Unfortunately, it has not yet been possible to detect any movement.

6. Conclusions

Bright/dark line alternance in cholesteric cyclic copolysiloxanes has been observed in solution-prepared and microtomed specimens by transmission electron microscopy. These lines are in accordance with the cholesteric pitch periodicity and are therefore perpendicular to the cholesteric axis. It has been demonstrated that the bright/dark line alternance could be explained by electron diffraction contrast which is destroyed by radiation damage of solution-prepared specimens. This contrast is related to the cholesteric packing of the mesogenic side chains. In the dark lines, it seems that the side chains lie in the substrate plane and are parallel to the lines. It is likely that they are perpendicular to the substrate plane in the bright lines.

After radiation damage, the contrast disappears in solution-processed specimens and increases in ultramicrotomed samples, probably because of a differential etching, which may be influenced by some sort of channelling. Our calculations indicate that the orientation of the molecule had no effect on the scattering molecular factor, so that if the orientation of the molecule does play a role, it must be sought in the distribution of lateral packing distances, and not in the molecular factor.

Specimens prepared from solution are easy to prepare and suitable for transmission electron microscopy. Fingerprint textures and spirals can be seen, with numerous disclinations and edge dislocations of different types. The carbon surface and the small thickness must play a role in the occurrence of these morphologies. For instance these factors must be taken into account in order to explain why the cholesteric axis is in the substrate plane, and why spirals occur so frequently.

We thank J. Bilotte and C. Jouret for their contribution to the observations on the CEMES high voltage microscope, and the referee for his profitable comments. We also thank F. H. Kreuzer for providing the polysiloxane samples.

References

[1] Shibaev, V. P., and Freidzon, Y. S., 1989, *Side Chain Liquid Crystal Polymers*, edited by C. B. McArdle (Blackie), p. 260.
[2] Mitov, M., and Sixou, P., 1993, *Molec. Crystals liq. Crystals*, **231,** 11.
[3] Noël, C., 1985, *Recent Advances in Liquid Crystalline Polymers*, edited by L. L. Chapoy (Elsevier Applied Science Publishers), p. 135.
[4] Bouligand, Y., and Kleman, M., 1970, *J. Physique*, **31,** 1041.
[5] Bouligand, Y., and Livolant, F., 1984, *J. Physique*, **45,** 1899.
[6] Hara, H., Satoh, T., Toya, T., Iida, S., Orii, S., and Watanabe, J., 1988, *Macromolecules*, **21,** 14.
[7] Dave, V., Glasser, W. G., and Wilkes, G. L., 1992, *Polymer Bull.*, **29,** 565.
[8] Bunning, T. J., Vezie, D. L., Lloyd, P. F., Haaland, N. D., Thomas, E. L., and Adams, W. W., 1994, *Liq. Crystals*, **16,** 769.
[9] Costello, M. J., Meiboom, S., and Sammon, M., 1984, *Phys. Rev.* A, **29,** 2957.
[10] Lydon, J. E., and Robinson, D. G., 1972, *Biochim. Biophys. Acta*, **260,** 298.
[11] Livolant, F., and Bouligand, Y., 1989, *Molec. Crystals liq. Crystals*, **166,** 91.
[12] Giasson, J., Revol, J. F., Ritcey, A. M., and Gray, D. G., 1988, *Biopolymers*, **27,** 1999.
[13] Gilli, J. M., Kamaye, M., and Sixou, P., 1991, *Molec. Crystals liq. Crystals*, **199,** 79.
[14] Bunning, T. J., Klei, H. E., Samulski, E. T., Crane, R. L., and Linville, R., 1991, *Liq. Crystals*, **10,** 445.

[15] KREUZER, F. H., 1981, *Proceedings 11. Freiburger Arbeitstagung Flussigkristalle*, 5.
[16] KREUZER, F. H., GAWHARY, M., WINKLER, R., and FINKELMANN, H., 981, E. P. 0060335.
[17] KREUZER, F. H., ANDREJEWSKI, D., HAAS, W., HABERLE, N., RIEPL, G., and SPES, P., 1991, *Molec. Crystals liq. Crystals*, **199,** 345.
[18] PINSL, J., BRAUCHLE, C., and KREUZER, F. H., 1987, *J. molec. Electron.*, **3,** 9.
[19] TSAI, M. L., CHEN, S. H., and JACOBS, S. D., 1989, *Appl. Phys. Lett.*, **54,** 2395.
[20] HEBERLE, H. J., MILLER, A., and KREUZER, F. H., 1989, *Liq. Crystals*, **5,** 907.
[21] MITOV, M., and SIXOU, P., 1992, *J. Phys. II* (*France*), **2,** 1659; MITOV, M., and SIXOU, P., 1995, *Int. J. Modern Phys. Lett.* B (in the press).
[22] TOURNIER-LASSERVE, V., BOUDET, A., and SOPENA, P., 1995, *Ultramicroscopy*, **58,** 123.
[23] BOUDET, A., and KUBIN, L. P., 1982, *Ultramicroscopy*, **8,** 409.
[24] BOUDET, A., 1984, *J. mater. Sci.*, **19,** 2989.
[25] BOUDET, A., and ROUCAU, C., 1985, *J. Physique*, **46,** 1571.
[26] KLEMAN, M., 1977, Point. Parois. Lignes (Les Editions de Physique), Tome I.
[27] DOYLE, P. A., and TURNER, P. S., 1968, *Acta Cryst.* A, **24,** 390.